Real-time MR Imaging With Gadoteridol Predicts Distribution of Transgenes After Convection-enhanced Delivery of AAV2 Vectors

Xiaomin Su[1], Adrian P Kells[1], Ernesto Aguilar Salegio[1], R Mark Richardson[1], Piotr Hadaczek[1], Janine Beyer[1], John Bringas[1], Philip Pivirotto[1], John Forsayeth[1] and Krystof S Bankiewicz[1]

[1]*Department of Neurological Surgery, University of California San Francisco, San Francisco, California, USA*

Gene therapies that utilize convention-enhanced delivery (CED) will require close monitoring of vector infusion in real time and accurate prediction of drug distribution. The magnetic resonance imaging (MRI) contrast agent, Gadoteridol (Gd), was used to monitor CED infusion and to predict the expression pattern of glial cell line-derived neurotrophic factor (GDNF) protein after administration of adeno-associated virus type 2 (AAV2) vector encoding human pre-pro-GDNF complementary DNA. The nonhuman primate (NHP) thalamus was utilized for modeling infusion to allow delivery of volumes more relevant to planned human studies. AAV2 encoding human aromatic L-amino acid decarboxylase (AADC) was coinfused with AAV2-GDNF/Gd to confirm regions of AAV2 transduction versus extracellular GDNF diffusion. There was a close correlation between Gd distribution and GDNF or AADC expression, and the ratios of expression areas of GDNF or AADC versus Gd were both close to 1. Our data support the use of Gd and MRI to monitor AAV2 infusion via CED and to predict the distribution of GDNF protein after AAV2-GDNF administration.

Received 5 January 2010; accepted 6 May 2010; published online 15 June 2010. doi:10.1038/mt.2010.114

INTRODUCTION

A key issue for gene therapy in the central nervous system is accurate and predictable anatomical localization of vector delivery. A series of potential problems with parenchymal infusions include leakage of infusate into cerebrospinal fluid spaces that prevents effective tissue distribution, reflux along the cannula tract that leads to exposure of vector to the peripheral immune system, and incorrect cannula placement in the target structure that leads to untoward distribution of transgene; all present real risks to patients. The development of visually monitored infusion platforms should significantly reduce these risks. Recent clinical trials of neurotrophic factor therapy for the treatment of Parkinson's disease, via direct delivery of recombinant glial cell-derived neurotrophic factor (GDNF) or a viral vector encoding Neurturin, have failed to demonstrate clinical benefit.[1,2] The discordant results within patient cohorts and across clinical trials are possibly due to poor or inappropriate distribution of the infusate within the target region.[3] Thus, without a fully optimized delivery system broadly usable by neurosurgeons, any clinical development program may be doomed, no matter how powerful the scientific rationale for therapeutic efficacy may have been.

The aim of the present study is to develop a method for enhanced safety and predictability in the delivery of adeno-associated virus type 2 (AAV2)-based gene therapy vectors to any target region. Specifically, this study is centered on a method for predicting AAV2-mediated GDNF expression volumes and patterns in the human striatum by correlating the distribution of coinfused MRI tracer, Gadoteridol (Gd, Prohance) with that of expressed GDNF. Coinfusion of Gd and AAV2-GDNF allows real-time monitoring of infusions via repeated MRI T1 sequences.

Preclinical studies of putaminal delivery of AAV2-GDNF via convection-enhanced delivery (CED) to aged and parkinsonian nonhuman primates (NHP) have proven that the putamen is the ideal delivery region for this gene therapy strategy.[4,5] However, since the putamen of Parkinson's disease patients is approximately fivefold larger than the parkinsonian NHP putamen,[6] the infusion volume in this study was scaled up to model the volumes required for coverage of the human putamen in clinical trials. Therefore, to approximate better the infusion parameters involved in optimal coverage of the human putamen, we targeted the NHP thalamus, which is ~1.4 times the size of the NHP putamen but comparable to putamen in terms of proximity to surrounding structures.[6] Thus, in the present study, we infused AAV2-GDNF vector at clinically relevant volumes (~150 µl) to the NHP thalamus to correlate patterns of Gd distribution with subsequent GDNF expression on histological sections.

Previous studies have shown that cerebral AAV2-GDNF infusion resulted not only in intracellular neuronal somata and fiber staining but also in extracellular immunoreactivity,[7] suggesting that transgene-derived GDNF protein is released into the extracellular space. This raised the possibility that extracellular GDNF protein may distribute in part via concentration gradient-mediated diffusion. Thus, the distribution of GDNF may be affected, not only by AAV2 vector convection and transduction, but possibly also by extracellular GDNF protein diffusion. To better differentiate virus

Correspondence: *Krystof S Bankiewicz, Department of Neurological Surgery, University of California San Francisco, San Francisco, California 94103, USA. E-mail: Krystof.Bankiewicz@ucsf.edu*

transduction versus GDNF protein diffusion, we coinfused a second AAV2 vector to express a nonsecreted, intracellular molecule, aromatic L-amino acid decarboxylase (AADC), with AAV2-GDNF/Gd. Because endogenous AADC is normally absent in the NHP thalamus,[8] the expression of transduced AADC in the thalamus predicts the boundary of AAV2 vector transduction and distribution.

RESULTS

Gd distribution in the thalamus

In this study, three rhesus primates were infused with ~150 µl (V_i) AAV2-GDNF/Gd (1–1.2 × 10^{12} vg/ml, n = 5) to the thalamus; three of these infusions included AAV2-AADC (1 × 10^{12} vg/ml, n = 3) (**Table 1**). Magnetic resonance imaging (MRI) was performed before and during the infusion. Coronal brain images separated by 1-mm intervals were obtained to evaluate the distribution of Gd (V_d).

T1-weighted MRI was performed at 5-minute intervals and the images showed that the anatomical region with Gd infusion was clearly distinguishable from the surrounding noninfused tissue (**Figure 1a,e**). At the beginning of the infusion, a cylinder of Gd formed around the tip of the cannula (**Figure 1a**). Infusion expanded radially to assume a more spherical pattern as the volume of infusion (V_i) was increased (**Figure 1b–e**). Quantitative reconstructions of Gd distribution in 3D at the end of infusion with OsiriX software showed a tear-drop-shaped signal (**Figure 1f**), and the final distribution volume ranged from 700 to 900 mm^3.

Correlation of Gd with GDNF histology

Animals were euthanized 5 weeks after vector infusion. Brain blocks containing the thalamus were postfixed and sectioned coronally. Sets of serial sections 0.8 mm apart were stained with an antibody against GDNF. Immunohistochemical analysis demonstrated that the expression pattern of GDNF protein around the infusion site was similar to Gd distribution (**Figure 2a,b**). A quantitative analysis showed that the areas of GDNF expression were highly correlated with those of Gd distribution (**Figure 2d,e**). The average ratio of GDNF staining areas versus Gd distribution areas was 1.08 ± 0.17. Highly magnified microscopic images demonstrated GDNF staining in the cytoplasm of neuronal cells as well as an extracellular staining pattern suggestive of GDNF binding to extracellular matrix (**Figure 2c**).

In addition, robust GDNF staining was observed in distinct cortical regions, far from the cannula tract, in all animals after thalamic AAV2-GDNF infusion (**Figures 2b, 3b,** and **4b**). We also found AADC staining in the cortex of NHP coinfused with AAV2-AADC (**Figures 3c** and **4c**). The presence of GDNF or AADC protein in the cortex was due to axonal transport from the thalamus.[9] Thus, in the present study, we excluded the staining in thalamocortical fibers and cortex from measured areas of gene expression in order to better compare Gd distribution with GDNF or AADC expression derived primarily from direct convective delivery within the thalamus.

It should be noted that one infusion (left hemisphere of NHP #1) showed reflux of AAV2-GDNF/Gd along the cannula track to the cortex (**Figure 2a,b**). This reflux was due to intraoperative repositioning of the cannula early in the infusion. All the other infusions displayed no sign of vector reflux. Because the reflux happened at the very end of the infusion, the leakage

Table 1 Experimental design

	Thalamus	
Primate	**Left side**	**Right side**
#1	AAV2-GDNF/Gd	AAV2-GDNF/Gd
#2	—	AAV2-GDNF/ AAV2-AADC/Gd
#3	AAV2-GDNF/ AAV2-AADC/Gd	AAV2-GDNF/ AAV2-AADC/Gd

Abbreviations: AAV2, adeno-associated virus type 2; AADC, aromatic L-amino acid decarboxylase; Gd, Gadoteridol; GDNF, glial cell line-derived neurotrophic factor.

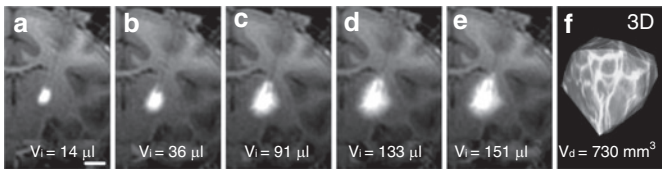

Figure 1 T1-weighted MR images with Gd RCD and 3D construction of ROI. (**a–e**) A series of real-time T1-weighted MR images in the coronal plane obtained at various times from the beginning to the end of infusion into the thalamus of one NHP. The volume of infusate (V_i) at the corresponding infusion time point is indicated at the bottom of each panel. Bar = 0.5 cm. (**f**) A 3D reconstruction of ROI based on Gd signal in the left thalamus after infusion. The volume of Gd distribution (V_d) is indicated at the bottom of the panel. AAV2, adeno-associated virus type 2; Gd, Gadoteridol; MR images, magnetic resonance images; NHP, nonhuman primate; RCD, real-time convective delivery; ROI, region of interest.

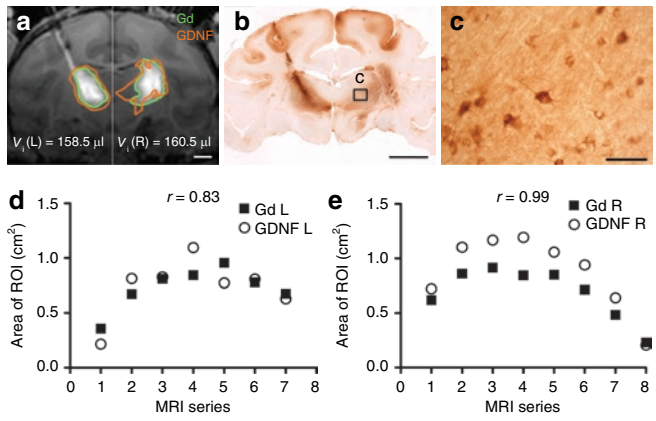

Figure 2 MRI correlation with histology in primate #1 with bilateral infusion of AAV2-GDNF into the thalamus. (**a**) A T1-weighted MR image of Gd distribution in the thalamus (green outline). Areas staining positive for GDNF (orange outline) of corresponding sections were transferred to the MR image for comparison. Since the left and right infusions were completed by different times, the final series of MR images for each infusion was cropped and merged in **a**. Infusion volume to the left and right brain was indicated at the bottom of the panel [V_i (L) and V_i (R)]. Bar = 0.5 cm. (**b**) Coronal histology of primate brain imaged in **a** shows GDNF staining in a pattern similar to that noted on MRI with Gd. Bar = 1 cm. (**c**) High magnification of boxed insert in **b**, showing GDNF-positive cells within the thalamus. Bar = 50 µm. (**d**,**e**) Areas of Gd distribution and GDNF expression on the (**d**) left and (**e**) right side of the brain in a series of MR images. AAV2, adeno-associated virus type 2; Gd, Gadoteridol; GDNF, glial cell line-derived neurotrophic factor; MRI, magnetic resonance imaging; *r*, correlation coefficient; ROI, region of interest.

of GDNF in this primate was very slight and, hence, did not substantially affect the outcome measurement.

Correlation of GDNF and AADC histology

Thalamic delivery of AAV2-GDNF resulted in robust intracellular and extracellular GDNF immunoreactivity. Given the equally broad distribution of MRI tracer Gd, the considerable GDNF distribution in the present study may be attributed to effective convection of infused vector (~150 µl). However, some degree of the distribution may also be attributed to extracellular diffusion of GDNF. Thus, in order to assess the effect of extracellular diffusion on the total area of gene expression, areas of GDNF expression were compared to areas of intracellular molecule AADC expression in animals with coinfusion of AAV2-AADC. In this way, cell transduction versus secretion and diffusion of the gene product could be differentiated.

Two primates (#2 and #3) were coinfused with AAV2-GDNF and AAV2-AADC into the thalamus; one (#2) received a unilateral infusion and the other (#3) bilateral. Adjacent brain sections containing thalamic infusions were stained for GDNF and AADC, respectively. In addition, since AADC immunostaining can detect both transduced and endogenous AADC in the NHP (**Figure 3c,e**), we developed a double chromogenic staining method to differentiate transduced AADC from endogenous AADC colocalized with tyrosine hydroxylase (TH)-positive neurons. Sections were stained both for AADC in light brown and for endogenous TH in bright red (**Figure 3d**). Nearly all neurons that contained endogenous AADC were also positive for TH.[8] Thus, cells containing endogenous AADC as well as TH were double-labeled and stained in dark red (**Figure 3f**) and only those transduced neurons with exogenous AADC were stained light brown with the single chromagen (**Figure 3i**). By superimposing the adjacent AADC-stained sections with AADC/TH dual-stained sections, we were able to delineate the boundary of transduced AADC expression (**Figure 3c**, blue line).

The unilateral coinfusion of AAV2-GDNF and AAV2-AADC into the thalamus of one primate (#2) allowed clear differentiation of endogenous and transduced AADC, because transduced AADC was only observed on the infused side of the brain. In contrast, endogenous AADC, colocalized with TH, was present bilaterally in the caudate, putamen, and substantia nigra (**Figure 3d**). For this particular primate, since the thalamic infusion extended to the medial aspect of putamen, AADC-positive cells were found at the edge of medial putamen (**Figure 3h**), in contrast to the left putamen that contained only endogenous AADC-positive fibers (**Figure 3g**). These AADC-positive cells in the right putamen were included in area measurements outlined in blue (**Figure 3h**).

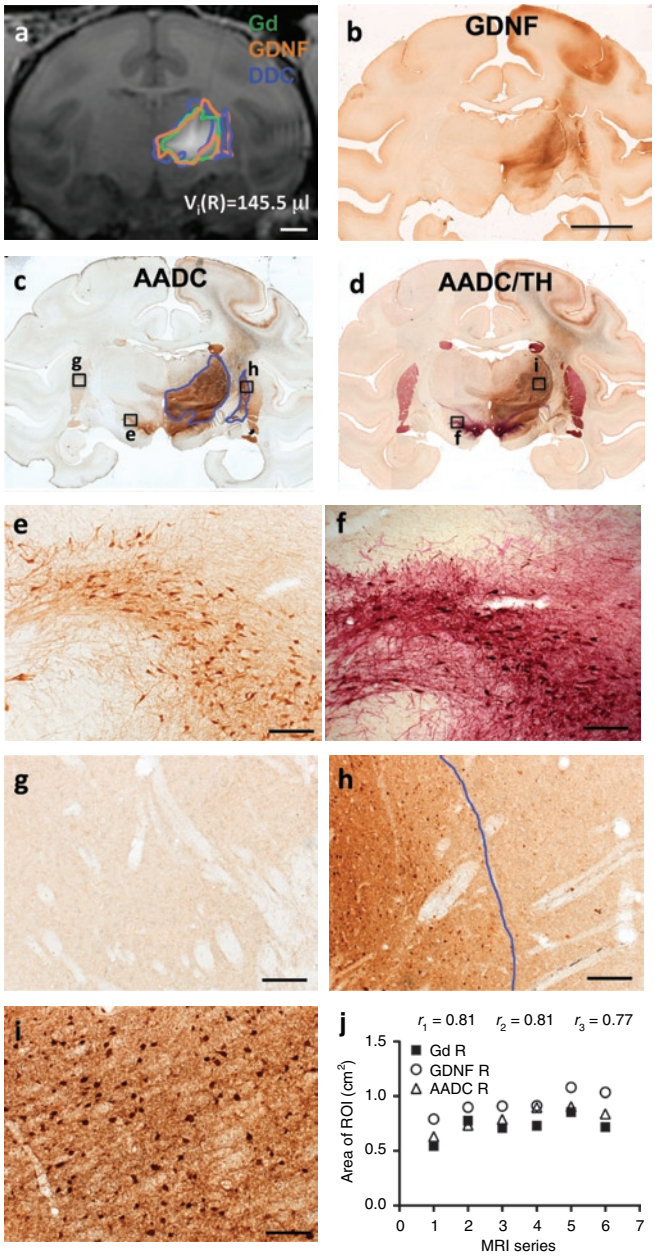

Figure 3 MRI correlation with histology in primate #2 with unilateral coinfusion of AAV2-GDNF and AAV2-AADC into the thalamus. (**a**) T1-weighted MR image showing Gd distribution in the thalamus (green outline). Areas staining positive for GDNF (orange outline) and AADC (blue outline) of corresponding sections were transferred to the MR image for comparison. Bar = 0.5 cm. (**b**) Coronal section of primate brain imaged in **a**, showing GDNF staining in a pattern similar to that noted on MRI with Gd. Bar = 1 cm. (**c**) AADC-stained section adjacent to (**b**), showing both endogenous and transduced AADC expression. Transduced AADC is outlined in blue. (**e**) AADC and TH colabeled section adjacent to (**c**), showing costaining for AADC in brown and tyrosine hydroxylase (TH) in red to differentiate endogenous AADC/TH (dark red) from transduced AADC (brown). The expression pattern of transduced AADC is nearly identical to GDNF expression in **b**. (**e**) High magnification of boxed insert in **c** showing endogenous AADC-positive cells in the nigra. Bar = 50 µm. (**f**) High magnification of boxed insert in **d** showing AADC/TH-positive cells in the nigra. Bar = 50 µm. (**g**) High magnification of boxed insert in **c** showing endogenous AADC-positive fibers in the putamen. Bar = 50 µm. (**h**) High magnification of boxed insert in **c** showing AADC-positive cells in the putamen. Bar = 50 µm. (**i**) High magnification of boxed insert in **d** showing AADC-positive cells in the thalamus. Bar = 50 µm. (**j**) The areas of Gd, GDNF, and AADC distribution on the right side of the brain in a series of MR images. AADC, aromatic L-amino acid decarboxylase; AAV2, adeno-associated virus type 2; Gd, Gadoteridol; GDNF, glial cell line-derived neurotrophic factor; MRI, magnetic resonance imaging; r_1, correlation coefficient between areas of Gd and GDNF expression; r_2, correlation coefficient between areas of Gd and AADC expression; r_3, correlation coefficient between areas of GDNF and AADC expression.

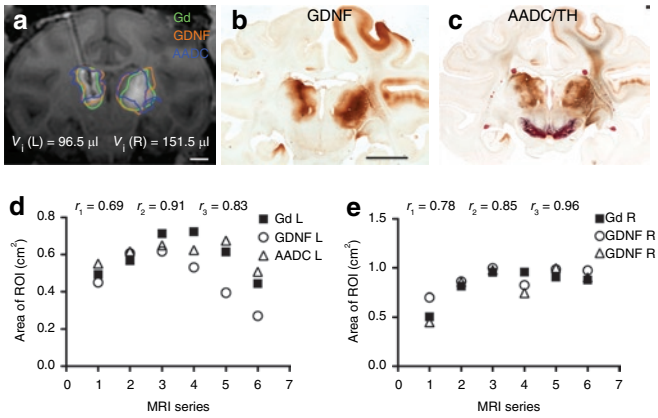

Figure 4 MRI correlation with histology in primate #3 with bilateral coinfusion of AAV2-GDNF and AAV2-AADC into the thalamus. (**a**) T1-weighted MR image showing Gd distribution in the thalamus, outlined in green. Areas staining positive for GDNF (outlined in orange) and AADC (outlined in blue) of corresponding sections were transferred to the MR image for comparison. Bar = 0.5 cm. (**b**) Coronal section of primate brain imaged in **a**, showing GDNF staining in a pattern similar to that noted on MRI with Gd. Bar =1 cm. (**c**) AADC and TH colabeled section adjacent to (**b**), showing costaining for AADC in brown and tyrosine hydroxylase (TH) in red. (**d**, **e**) Areas of Gd, GDNF, and AADC distribution on the (**d**) left and (**e**) right side of the brain in a series of MR images. AADC, aromatic L-amino acid decarboxylase; AAV2, adeno-associated virus type 2; Gd, Gadoteridol; GDNF, glial cell line-derived neurotrophic factor; MRI, magnetic resonance imaging; r_1, correlation coefficient between areas of Gd and GDNF expression; r_2, correlation coefficient between areas of Gd and AADC expression; r_3, correlation coefficient between areas of GDNF and AADC expression.

The overall intensity of AADC staining in the right putamen and caudate appeared greater than in the corresponding left side (**Figure 3c,g,h**). We also observed a similar pattern in sections stained for GDNF (**Figure 3b**). The enhanced AADC- or GDNF staining in the right putamen and caudate was probably due to anterograde transport of expressed gene product from the dorsal nigra into which the infusion extended in this primate. Thus, these regions were not considered direct vector transduction areas and were excluded from the quantitative analysis.

By comparing the adjacent GDNF and AADC/TH stained sections, we observed that the expression patterns of GDNF and exogenous AADC in the thalamus were nearly identical. In addition, GDNF and AADC expression substantially overlapped with Gd distribution (**Figure 3a**). The areas of Gd, GDNF, and AADC distribution in a series of coronal planes were highly correlated with one another (**Figure 3j**). The mean ratio of AADC staining areas versus Gd distribution areas was 1.07 ± 0.06, identical to GDNF versus Gd (1.08 ± 0.17). All of these data strongly indicated an excellent match between AADC and GDNF distribution.

Bilateral coinfusion of AAV2-GDNF and AAV2-AADC into the thalamus of another primate (#3) further validated our findings (**Figure 4**). The majority of transduced GDNF and AADC protein was confined to both sides of thalamus (**Figure 4b,c**), where expression patterns closely correlated with Gd distribution (**Figure 4a,d,e**).

DISCUSSION

In the present study, we used an MRI contrast agent to visualize the infusion in real time in order to predict the distribution of a therapeutic agent AAV2-GDNF. The NHP thalamus was utilized for modeling infusions in the human putamen to allow delivery of clinically relevant volumes. We were able to administer vector at a V_i of ~150 µl into the thalamus by CED without significant reflux or leakage (excluding, of course, the one instance in which a cannula was repositioned). There was an excellent correlation between Gd distribution and both AAV2-GDNF and AAV2-AADC expression and the ratios of expression areas of GDNF or AADC versus Gd were both close to 1, strongly suggesting that we can predict the distribution of AAV2 transduction and subsequent gene expression with contrast (Gd) MRI. In addition, since the expression patterns of GDNF and AADC are identical, there was no detectable diffusion of GDNF protein after AAV2-GDNF transduction. In this study, one primate received a bilateral infusion of AAV2-GDNF vector only, and the other two received the coinfusion of AAV2-GDNF and AAV2-AADC. Given the excellent match between Gd distribution and AAV2-GDNF expression in all these primates regardless of the infusion pattern, there was no significant effect of coinfusion of AAV2-AADC on the spread of AAV2-GDNF. Therefore, coinfusion of the intracellular marker AAV2-AADC offers a reliable prediction of AAV2-GDNF vector transduction.

Infusion of powerful therapies directly into disease-affected regions of the human brain with CED provides an effective strategy for treating neurological disorders.[10–14] Although CED can be used for broad therapeutic distribution over large brain regions, continuous administration could cause undesired effects due to leakage of infusate into subarachnoid and ventricular spaces.[15,16] In fact, in a separate study, we recently found that one of our parkinsonian primates with putaminal infusion of AAV2-GDNF displayed L-dopa-induced dyskinesia and weight-loss as a result of leakage of GDNF outside the targeted region (K.S. Bankiewicz, unpublished results). Therefore, clinical trials that utilize CED will require close monitoring of drug infusion and accurate prediction of drug distribution. In the present study, coinfusion of the MRI contrast agent, Gd, with AAV2-GDNF proved to be useful in monitoring infusion and estimating therapeutic distribution. Real-time MRI with Gd clearly revealed an effective infusion region distinguishable from surrounding tissue (**Figure 1a–e**). This well-defined infusion region allowed for real-time adjustment of infusion parameters and precise volumetric analysis.

The distribution of infusate by CED is determined by many factors, such as particle size, particle surface property, dose, and tissue binding.[17–20] Gd, by virtue of its smaller particle size (~2 nm in diameter), might be expected to transport faster through brain tissue than AAV2 vector (24–26 nm diameter). However, during CED, the difference in distribution between Gd and AAV vector is slight,[21,22] probably due to the predominant driving force of pressure gradient-mediated fluid advection rather than concentration gradient-mediated diffusion. Thus, MRI Gd signal reliably mimics the distribution of AAV2 vector during infusion. Over longer time scales, the distribution of AAV2 vector, as well as extracellular GDNF released by transduced cells in the brain, may depend solely on the concentration gradient and the diffusivity of the infusate in the tissue. The diffusion rate for high-molecular weight compounds, including gene therapy vectors and growth factors in brain tissues is extremely low.[23] In addition, AAV2 vector and GDNF protein

bind heparin components in heparin-sulfate proteoglycans on cell wall and extracellular matrix within the interstitial space,[24–26] perhaps substantially limiting their spread via diffusion. We found that the distribution of Gd and GDNF expression 5 weeks after infusion were approximately equal. Furthermore, the distribution of GDNF was very similar to that of the intracellular enzyme, AADC. These findings were consistent with previous studies[23,27] and strongly suggestive of limited diffusion of AAV2 vector or GDNF after infusion. Therefore, the distribution of CED infusion of Gd may effectively predict the distribution of AAV2-GDNF both acutely and over longer time periods.

In summary, we infused AAV2-GDNF vector accurately to primate thalamus via CED with real-time MRI imaging. Contrast MRI provides a valuable tool to guide AAV2 vector infusion and predicts AAV2-GDNF distribution reliably, allowing for increased safety, precision, and clinically relevant coverage of the putamen with this vector in Parkinson's disease patients.

MATERIALS AND METHODS

Experimental subjects and study design. Three normal adult rhesus macaques (NHP) were used in the present study. Experimentation was performed according to the National Institutes of Health guidelines and to the protocols approved by the Institute Animal Care and Use Committee at the University of California San Francisco (San Francisco, CA). The three NHP received intracranial infusions of AAV2 vectors and free Gd (1 mmol/l Gd, Prohance; Bracco Diagnostics, Princeton, NJ) into the thalamus. Infusions were performed by previously established CED techniques for NHP.[3]

Infusion formulation. AAV2 vectors containing complementary DNA sequences for either human GDNF (AAV2-GDNF) or human AADC (AAV2-AADC) under the control of the cytomegalovirus promoter were packaged by the AAV Clinical Vector Core at Children's Hospital of Philadelphia as previously described.[28,29] AAV2-GDNF and AAV2-AADC stocks were diluted immediately before use to equivalent titers of 1–1.2 × 10^{12} vector genomes/ml in phosphate-buffered saline with 0.001% (vol/vol) Pluronic F-68.

Infusion procedure. NHP underwent neurosurgical procedures to position MRI-compatible guide arrays over the thalamus. Each customized guide array was cut to a specified length, stereotactically guided to its target through a burr-hole created in the skull and secured to the skull by dental acrylic. The tops of the guide array assemblies were capped with stylet screws for simple access during the infusion procedure. Animals recovered for at least 2 weeks before initiation of infusion procedures.

NHP were sedated as previous studies mentioned.[5] Each animal's head was placed in an MRI-compatible stereotactic frame, and a baseline MRI was performed before infusion to visualize anatomical landmarks and to generate stereotactic coordinates of the proposed target infusion sites for each animal. Vital signs, such as heart rate and PO2, were monitored throughout the procedure. Briefly, the infusion system consisted of a fused silica reflux-resistant cannula with a 3-mm step[30,31] that was connected to a loading line (containing vectors and Gd), an infusion line with oil and another infusion line with Trypan blue solution. A 1-ml syringe (filled Trypan blue solution) mounted onto a microinfusion pump (BeeHive; Bioanalytical System, West Lafayette, IN) regulated the flow of fluid through the system. Based on MRI coordinates, the cannula was manually guided to the targeted region of the brain through the previously placed guide array. The 3-mm step at the tip of the cannula was designed to maximize fluid distribution during CED procedures and minimize reflux along the cannula tract. After securing placement of the infusion cannula, the CED procedures with acquisition of real-time MRI data (real-time convective delivery) were initiated. We used the same infusion parameters for every NHP infused throughout the study. Infusion rates were as follows: 1 µl/min was applied when lowering cannula to targeted area and increased at 20–30-min intervals to 1.5 and 2.0 µl/min. After infusion, the cannula was withdrawn from the brain and the animals were allowed to recover under close observation until able to right themselves in their home cages.

MRI. MR images of brain were acquired on a 1.5-T Siemens Magnetom Avanto (Siemens AG, Munich, Germany). Three-dimensional rapid gradient echo (MP-RAGE) images were obtained with repetition time = 17 ms, echo time = 4.5 ms, flip angle = 15°, number of excitations = 1 (repeated three times), matrix = 256 × 256, field of view = 240 × 240 × 240 and slice thickness = 1 mm. These parameters resulted in a 1-mm^3 voxel volume. The scanning time was ~5 minutes per sequence with continuous scanning throughout the infusion procedure.

Volume and area quantification of Gd distribution from MR images. The volume of Gd distribution within each infused brain region was quantified with OsiriX Medical Image software (v. 3.6; OsiriX Foundation, Geneva, Switzerland). The software reads all data specifications from MR images. After the pixel threshold value for Gd signal is defined, the software calculates the signal above a defined threshold value, and establishes the area of region of interest for each MRI series and computes the distribution volume V_d of region of interest for the NHP brain. This allows V_d to be determined at any given time point and can be reconstructed in a three-dimensional image.

Histological procedures. Animals were deeply anesthetized with sodium pentobarbital (25 mg/kg intravenous) and euthanized ~5 weeks after vector administration. The brains were harvested and coronally sliced with a brain matrix. The brain blocks were postfixed with 4% paraformaldehyde and then cut into 40-µm coronal sections in a cryostat. Sections were processed for immunohistochemistry staining. Serial sections were stained for GDNF and AADC. Every 20th section was washed in phosphate-buffered saline and incubated in 1% H_2O_2 vol/vol for 20 minutes to block endogenous peroxidase activity. After washing sections in phosphate-buffered saline, they were incubated in Sniper blocking solution (Biocare Medical, Concord, CA) for 30 minutes at room temperature followed by incubation with primary antibodies (GDNF, 1:500, R&D Systems, Minneapolis, MN; AADC, 1:1,000, Chemicon, Billerica, MA; TH, 1:10000, Chemicon) in Da Vinci diluent (Biocare Medical) overnight at room temperature. After three rinses in phosphate-buffered saline for 5 minutes each at 22–24 °C, sections were incubated in Mach 2 or Goat HRP polymer (Biocare Medical) for 1 hour at 22–24 °C, followed by several washes and colorimetric development (DAB; Vector Laboratories, Burlingame, CA; Vulcan Fast Red; Biocare Medical). Immunostained sections were mounted on slides and sealed with Cytoseal (Richard-Allan Scientific, Kalamazoo, MI).

Area qualification of GDNF and AADC expression. The analysis of GDNF and AADC expression was performed with a Zeiss light microscope. GDNF- and AADC-positive areas were identified at low magnification and positively stained cells were confirmed under high magnification. Because intracellular and extracellular GDNF was present, it was difficult to determine GDNF staining areas based on positive cells. Therefore, low magnification GDNF stained images were analyzed with Image J software and positively stained areas were identified with a threshold function. In contrast, the boundary of intracellular AADC staining areas were easy to delineate manually based on high-magnification microscope imaging. Areas staining positive for GDNF or AADC were transferred to the corresponding primate MRI by manually delineating positive areas on the corresponding baseline MRI images using OsiriX software without reference to the MR images showing Gd distribution.

Statistical analysis. The areas of Gd distribution, GDNF or AADC expression were compared by Student's *t*-test and Pearson's correlation test. The criterion for statistical significance for all tests was $P < 0.05$.

ACKNOWLEDGMENTS

This study was supported by research grants from the Michael J. Fox Foundation and a generous gift from the Kinetics Foundation. We also like to acknowledge the skilled technical assistance of Maria Bartola Mejia, Hannah Mirek, and Yuying Zhai.

REFERENCES

1. Lang, AE, Gill, S, Patel, NK, Lozano, A, Nutt, JG, Penn, R *et al.* (2006). Randomized controlled trial of intraputamenal glial cell line-derived neurotrophic factor infusion in Parkinson disease. *Ann Neurol* **59**: 459–466.
2. Nutt, JG, Burchiel, KJ, Comella, CL, Jankovic, J, Lang, AE, Laws, ER Jr *et al.* (2003). Randomized, double-blind trial of glial cell line-derived neurotrophic factor (GDNF) in PD. *Neurology* **60**: 69–73.
3. Yin, D, Valles, FE, Fiandaca, MS, Bringas, J, Gimenez, F, Berger, MS *et al.* (2009). Optimal region of the putamen for image-guided convection-enhanced delivery of therapeutics in human and non-human primates. *Neuroimage* (epub ahead of print).
4. Su, X, Kells, AP, Huang, EJ, Lee, HS, Hadaczek, P, Beyer, J *et al.* (2009). Safety evaluation of AAV2-GDNF gene transfer into the dopaminergic nigrostriatal pathway in aged and parkinsonian rhesus monkeys. *Hum Gene Ther* **20**: 1627–1640.
5. Eberling, JL, Kells, AP, Pivirotto, P, Beyer, J, Bringas, J, Federoff, HJ *et al.* (2009). Functional effects of AAV2-GDNF on the dopaminergic nigrostriatal pathway in parkinsonian rhesus monkeys. *Hum Gene Ther* **20**: 511–518.
6. Yin, D, Valles, FE, Fiandaca, MS, Forsayeth, J, Larson, P, Starr, P *et al.* (2009). Striatal volume differences between non-human and human primates. *J Neurosci Methods* **176**: 200–205.
7. Johnston, LC, Eberling, J, Pivirotto, P, Hadaczek, P, Federoff, HJ, Forsayeth, J *et al.* (2009). Clinically relevant effects of convection-enhanced delivery of AAV2-GDNF on the dopaminergic nigrostriatal pathway in aged rhesus monkeys. *Hum Gene Ther* **20**: 497–510.
8. Weihe, E, Depboylu, C, Schütz, B, Schäfer, MK and Eiden, LE (2006). Three types of tyrosine hydroxylase-positive CNS neurons distinguished by dopa decarboxylase and VMAT2 co-expression. *Cell Mol Neurobiol* **26**: 659–678.
9. Kells, AP, Hadaczek, P, Yin, D, Bringas, J, Varenika, V, Forsayeth, J *et al.* (2009). Efficient gene therapy-based method for the delivery of therapeutics to primate cortex. *Proc Natl Acad Sci USA* **106**: 2407–2411.
10. Cunningham, J, Oiwa, Y, Nagy, D, Podsakoff, G, Colosi, P and Bankiewicz, KS (2000). Distribution of AAV-TK following intracranial convection-enhanced delivery into rats. *Cell Transplant* **9**: 585–594.
11. Saito, R, Krauze, MT, Noble, CO, Drummond, DC, Kirpotin, DB, Berger, MS *et al.* (2006). Convection-enhanced delivery of Ls-TPT enables an effective, continuous, low-dose chemotherapy against malignant glioma xenograft model. *Neuro-oncology* **8**: 205–214.
12. Yamashita, Y, Krauze, MT, Kawaguchi, T, Noble, CO, Drummond, DC, Park, JW *et al.* (2007). Convection-enhanced delivery of a topoisomerase I inhibitor (nanoliposomal topotecan) and a topoisomerase II inhibitor (pegylated liposomal doxorubicin) in intracranial brain tumor xenografts. *Neuro-oncology* **9**: 20–28.
13. Krauze, MT, Noble, CO, Kawaguchi, T, Drummond, D, Kirpotin, DB, Yamashita, Y *et al.* (2007). Convection-enhanced delivery of nanoliposomal CPT-11 (irinotecan) and PEGylated liposomal doxorubicin (Doxil) in rodent intracranial brain tumor xenografts. *Neuro-oncology* **9**: 393–403.
14. Fiandaca, MS, Forsayeth, JR, Dickinson, PJ and Bankiewicz, KS (2008). Image-guided convection-enhanced delivery platform in the treatment of neurological diseases. *Neurotherapeutics* **5**: 123–127.
15. Sampson, JH, Brady, ML, Petry, NA, Croteau, D, Friedman, AH, Friedman, HS *et al.* (2007). Intracerebral infusate distribution by convection-enhanced delivery in humans with malignant gliomas: descriptive effects of target anatomy and catheter positioning. *Neurosurgery* **60**(2 Suppl 1): ONS89–98; discussion ONS98.
16. Varenika, V, Dickinson, P, Bringas, J, LeCouteur, R, Higgins, R, Park, J *et al.* (2008). Detection of infusate leakage in the brain using real-time imaging of convection-enhanced delivery. *J Neurosurg* **109**: 874–880.
17. Szerlip, NJ, Walbridge, S, Yang, L, Morrison, PF, Degen, JW, Jarrell, ST *et al.* (2007). Real-time imaging of convection-enhanced delivery of viruses and virus-sized particles. *J Neurosurg* **107**: 560–567.
18. Chen, MY, Hoffer, A, Morrison, PF, Hamilton, JF, Hughes, J, Schlageter, KS *et al.* (2005). Surface properties, more than size, limiting convective distribution of virus-sized particles and viruses in the central nervous system. *J Neurosurg* **103**: 311–319.
19. Kroll, RA, Pagel, MA, Muldoon, LL, Roman-Goldstein, S and Neuwelt, EA (1996). Increasing volume of distribution to the brain with interstitial infusion: dose, rather than convection, might be the most important factor. *Neurosurgery* **38**: 746–752.
20. Chen, MY, Lonser, RR, Morrison, PF, Governale, LS and Oldfield, EH (1999). Variables affecting convection-enhanced delivery to the striatum: a systematic examination of rate of infusion, cannula size, infusate concentration, and tissue-cannula sealing time. *J Neurosurg* **90**: 315–320.
21. Ding, D, Kanaly, CW, Bigner, DD, Cummings, TJ, Herndon, JE 2nd, Pastan, I *et al.* (2009). Convection-enhanced delivery of free gadolinium with the recombinant immunotoxin MR1-1. *J Neurooncol* (epub ahead of print).
22. Raghavan, R, Brady, ML, Rodríguez-Ponce, MI, Hartlep, A, Pedain, C and Sampson, JH (2006). Convection-enhanced delivery of therapeutics for brain disease, and its optimization. *Neurosurg Focus* **20**: E12.
23. Morrison, PF and Dedrick, RL (1986). Transport of cisplatin in rat brain following microinfusion: an analysis. *J Pharm Sci* **75**: 120–128.
24. Nguyen, JB, Sanchez-Pernaute, R, Cunningham, J and Bankiewicz, KS (2001). Convection-enhanced delivery of AAV-2 combined with heparin increases TK gene transfer in the rat brain. *Neuroreport* **12**: 1961–1964.
25. Qiu, J, Handa, A, Kirby, M and Brown, KE (2000). The interaction of heparin sulfate and adeno-associated virus 2. *Virology* **269**: 137–147.
26. Hamilton, JF, Morrison, PF, Chen, MY, Harvey-White, J, Pernaute, RS, Phillips, H *et al.* (2001). Heparin coinfusion during convection-enhanced delivery (CED) increases the distribution of the glial-derived neurotrophic factor (GDNF) ligand family in rat striatum and enhances the pharmacological activity of neurturin. *Exp Neurol* **168**: 155–161.
27. Aguilar Salegio, EA, Kells, AP, Richardson, M, Hadaczek, P, Forsayeth, J, Bringas, J *et al.* MRI-guided delivery of AAV2 to the primate brain for the treatment of lysosomal storage disorders. *Hum Gene Ther* (epub ahead of print).
28. Matsushita, T, Elliger, S, Elliger, C, Podsakoff, G, Villarreal, L, Kurtzman, GJ *et al.* (1998). Adeno-associated virus vectors can be efficiently produced without helper virus. *Gene Ther* **5**: 938–945.
29. Wright, JF, Qu, G, Tang, C and Sommer, JM (2003). Recombinant adeno-associated virus: formulation challenges and strategies for a gene therapy vector. *Curr Opin Drug Discov Devel* **6**: 174–178.
30. Krauze, MT, Mcknight, TR, Yamashita, Y, Bringas, J, Noble, CO, Saito, R *et al.* (2005). Real-time visualization and characterization of liposomal delivery into the monkey brain by magnetic resonance imaging. *Brain Res Brain Res Protoc* **16**: 20–26.
31. Krauze, MT, Saito, R, Noble, C, Tamas, M, Bringas, J, Park, JW *et al.* (2005). Reflux-free cannula for convection-enhanced high-speed delivery of therapeutic agents. *J Neurosurg* **103**: 923–929.